

Freely draining gravity currents in porous media: Dipole self-similar solutions with and without capillary retention

JOCHONIA S. MATHUNJWA and ANDREW J. HOGG

*Centre of Environmental and Geophysical Flows School of Mathematics,
University of Bristol University Walk, Bristol BS8 1TW, UK
email: a.j.hogg@bris.ac.uk*

(Received 30 March 2007)

We analyse the two-dimensional, gravitationally-driven spreading of fluid through a porous medium overlying a horizontal impermeable boundary from which fluid can drain freely at one end. Under the assumption that none of the intruding fluid is retained within the pores in the trail of the current, the motion of the current is described by the dipole self-similar solution of the first kind derived by Barenblatt and Zel'dovich (1957). We show that small perturbations of arbitrary shape imposed on this solution decay in time, indicating that the self-similar solution is linearly stable. We use the connection between the perturbation eigenfunctions and symmetry transformations of the self-similar solution to demonstrate that variables can always be specified in terms of which the rate of decay of the perturbations is maximised. Unsaturated flow can be modelled by assuming that a constant fraction of the fluid is retained within the pores by capillary action in the trail of the current. It has been shown (Barenblatt and Zel'dovich, 1998; Ingerman and Shvets, 1999) that in this case, the motion of the current is described by a self-similar solution of the second kind characterised by an anomalous exponent. We derive leading-order analytic expressions for the anomalous exponent and the self-similar quantities valid for small values of the fraction of fluid retained using direct asymptotic analysis and by using a novel application of the method of multiple scales. The latter offers a number of advantages and permits the evolution of the current to be clearly connected with its initial conditions in a way not possible with conventional approaches. We demonstrate that the theoretical predictions provided by these expressions are in excellent agreement with results from the numerical integration of the governing equations.

1 Introduction

Gravity-driven motion through porous media occurs in numerous environmental and industrial settings, driven by density gradients between the intruding and ambient fluids. Often in situations where the porous medium is of semi-infinite lateral extent, as the current spreads into the medium, part of the fluid freely drains out from the ends of the domain. Examples of such situations include groundwater flows that border rivers and oceans where, after flooding during high tide, water freely drains back at low tide, and the borders of a reservoir that may become contaminated when the reservoir is flooded and

bursts, but, as it spreads into the porous formation, the contaminated fluid also drains back when the reservoir level returns to normal.

In this paper, we study the two-dimensional motion of a gravity current that flows through a porous medium over an impenetrable horizontal boundary and drains freely from one end, subsequent to a finite release of dense fluid. We first consider a model for saturated flow in which it is assumed that there is no capillary retention of fluid within the pores wetted by the intruding fluid. Although the volume of the current is not constant in time, it has been shown by Barenblatt and Zel'dovich (1957) that provided the volume flux of the fluid draining out remains finite, a quantity termed the dipole moment of the current and defined below is conserved in time. Then the intermediate asymptotic development of current is described by a self-similar solution of the first kind (SS1). This dipole self-similar solution models the flow of currents through saturated porous media and its theoretical predictions have been found to be in excellent agreement with experimental results (King and Woods, 2003). Dipole moment preserving solutions have also been constructed in the rather different physical context of capillary-driven spreading of fluid droplets (see, for example, Bernis *et al.*, 2000; and Bowen and Witelski, 2006).

The purpose of the first part of this paper is to analyse the linear stability properties of the self-similar solution to the dipole-preserving flow with a porous domain. We impose a disturbance (perturbation) of arbitrary shape on the self-similar solution and perform a linearised analysis to determine the subsequent development of the system. The analysis reveals that all disturbance eigenfunctions decay in time at rates that may be calculated analytically and this establishes that the dipole self-similar solution is linearly stable. We then demonstrate the connection between the disturbance eigenfunctions and the symmetry transformations of the dipole self-similar solution, and show that optimal variables can always be found in terms of which the leading-order rate of decay of the disturbance is maximised.

When fluid flows through an unsaturated porous domain, a proportion of it may be retained in the wetted pores due to capillary action (see, for example, Bear, 1988; Barenblatt, 1996). The retention affects the motion – and, in particular, this implies that the dipole moment is no longer constant in time. Under the assumption that the fraction of fluid retained is constant (see, for example, Barenblatt, 1996), the intermediate asymptotic behaviour of the current is given by a dipole self-similar solution of the second kind (SS2). The fundamental governing equations of this fluid motion have been proposed by Barenblatt and Vazquez (1998), calculated numerically by Ingerman and Shvets (1999) and analysed in the regime of small retention by Wagner (2005). We remark that in general, while SS1 describes the intermediate asymptotics of problems that satisfy certain integral conservation laws, SS2 describes the intermediate asymptotics of problems for which these integral conservation laws no longer hold – and this is the situation for these flows. Furthermore, a characteristic trait of problems described by SS1 is that their intermediate asymptotic behaviour is independent of the precise initial conditions. Thus for this case, in the absence of retention, gravity currents with equal dipole moments but different initial height profiles will be indistinguishable in the intermediate regime. The self-similar exponents are determined by the use of dimensional analysis and the integral conservation law of the dipole moment. For problems described by SS2, the intermediate asymptotic behaviour is not completely independent of the initial conditions.

The use of dimensional analysis partially determines the similarity exponents in terms of a non-trivial anomalous exponent. The standard procedure of obtaining the remaining similarity parameters involves numerically solving an eigenvalue problem to determine the anomalous exponent, and matching with a numerical solution of the particular problem to specify the rest of the parameters. Thus for a given initial condition, although the similarity exponent may be calculated directly or by asymptotic means such as those developed by Goldenfeld *et al.* (1990) and Wagner (2005), it has not been possible to develop a complete description of the flow without recourse to numerical integration of the governing partial differential equations. In this paper, we suggest a means for avoiding these numerical calculations and yet still capturing the anomalous exponent that is the key feature of SS2.

In the second part of the paper, we study currents described by dipole SS2. We first calculate the similarity solutions numerically and obtain results similar to those found by Ingerman and Shvets (1999). We demonstrate that it is possible to evaluate the anomalous exponents in the regimes of weak and strong capillary retention, using direct asymptotic techniques that in the regime of weak retention recover results identical to those of Wagner (2005) without the need for more elaborate asymptotic strategies. Weak capillary retention modifies the motion over very long time scale relative to the inherent time scale of the flow. We exploit this separation by using the method of multiple scales to obtain the leading-order analytical expression for the anomalous similarity exponents, which is in accord with that calculated using other techniques, and the other similarity parameters. This approach improves on previous procedures of finding SS2 because it permits the evolution of the current in the self-similar regime to be related to the initial conditions in a way not possible with these techniques. Thus, it fully determines the similarity parameters and does not need to be supplemented by numerical calculations. Taken together, the two parts of this paper show how, if the capillary retention is weak and from given initial conditions, the motion first approaches that described by an SS1, defined solely by the initial dipole moment and then over much longer timescales is modified by retention entering a new spreading regime. This process is illustrated by the numerical integration of the governing partial differential equation from a particular initial condition and it is shown that the numerically calculated values are in excellent agreement with the theoretical predictions.

The paper is organised as follows. We consider currents with no capillary retention in section 2. The dipole SS1 is presented and generalised in section 2.1 for a current through a porous medium with permeability that is constant or varies with vertical distance. In section 2.2, we perform a new linear stability analysis and show that the dipole SS1 is linearly stable. The connection between the disturbance eigenfunctions and the symmetry transformations of the dipole SS1 is shown in section 2.3, where an estimate of the leading-order rate of decay of the disturbance is also made. Currents with capillary retention are considered in section 3. A numerical solution of the eigenvalue problem for the anomalous exponent and the dipole SS2 is presented in section 3.1. Then, in section 3.2, the leading-order analytic expressions for the anomalous exponent and the dipole SS2 are derived using the method of multiple scales. In section 4, we present a comparison between the theoretical predictions and numerical integration of the governing partial differential equations. A summary of the main findings of the paper is presented in section 5. We also

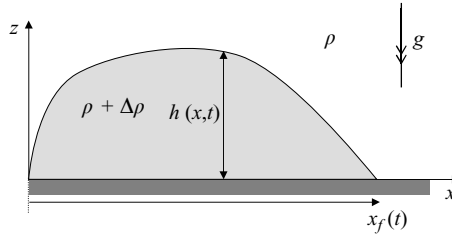


FIGURE 1. The configuration of the flow. The gravity current spreads through the porous medium, over the horizontal impermeable boundary and drains freely at $x = 0$.

include an appendix that applies direct asymptotic analysis of the equation governing the form of SS2 in the regimes of weak and strong retention of fluid to reveal the dependence of the anomalous exponent upon the fraction of fluid retained.

2 Currents with no capillary retention

We analyse the lateral spreading of a two-dimensional gravity current produced by the finite release of fluid in a semi-infinite porous medium overlying an impermeable horizontal boundary from which fluid can drain freely at one end. We assume that the porous medium is initially saturated with fluid of density ρ while the intruding fluid has density $\rho + \Delta\rho$. The geometry of the flow is illustrated in Figure 1. Thus, as the current spreads into the porous medium ($x > 0$), it simultaneously drains freely at $x = 0$. We also assume that the porous medium is homogeneous in horizontal directions, but varies vertically according to $K_0 z^{\alpha-1}$, where $K_0 > 0$ and $\alpha > 0$ are constants and z is the dimensionless vertical distance from the lower boundary. We consider the case where none of the fluid is retained within the pores by capillary action as the current flows and when the current is sufficiently shallow that the pressure adopts hydrostatic balance in the vertical direction.

Then, the motion of the shallow gravity current is governed by the porous medium equation,

$$\partial_t h = \kappa \partial_x (h^\alpha \partial_x h), \tag{2.1}$$

where h is the height of the current, $\kappa = K_0 \Delta\rho g / \mu$, g is the gravitational acceleration and μ is the dynamic viscosity (see, for example, Huppert & Woods, 1995; Barenblatt, 1996; King & Woods, 2003). We introduce a dimensionless time $\tau = t/t_0$ and nondimensionalise lengths with respect to $(\kappa t_0)^{1/(2-\alpha)}$, where $t = t_0$ is some reference initial time. The governing equation then becomes

$$\partial_\tau h = \partial_x (h^\alpha \partial_x h), \tag{2.2}$$

and the boundary conditions are given by

$$h(0, \tau) = 0, \tag{2.3}$$

$$h(x_F, \tau) = 0, \tag{2.4}$$

where $x_F(\tau)$ is the dimensionless position of the front of the current. These conditions

indicate that the height vanishes at the origin and at the front of the current, respectively. In addition, the volume flux per unit width, $q = h^\alpha \partial_x h$, is assumed to remain finite at the origin ($x = 0$) and vanish at the front ($x = x_F$).

The problem defined by equations (2.2)–(2.4) and the condition of vanishing flux at the front does not conserve the volume per unit width of the current as the fluid flows, because fluid drains out of the domain at $x = 0$. However, for the case $\alpha = 1$ corresponding to a porous medium with constant permeability, it has been shown by Barenblatt and Zel'dovich (1957) that the dipole moment \mathcal{M} defined by

$$\mathcal{M} = \int_0^{x_F} xh(x, \tau) dx \tag{2.5}$$

remains constant in time for these flows provided $q(0, \tau)$ is finite. It is straightforward to show that this property is satisfied by the problem for general values of $\alpha > 0$. Differentiating (2.5) with respect to τ and combining it with (2.2) yields

$$\begin{aligned} \frac{d}{d\tau} \int_0^{x_F} xh(x, \tau) dx &= \frac{dx_F}{d\tau} x_F h(x_F, \tau) + \int_0^{x_F} x \partial_\tau h dx \\ &= \int_0^{x_F} x \partial_x (h^\alpha \partial_x h) dx \\ &= [x(h^\alpha \partial_x h) - h^{\alpha+1}/(\alpha + 1)]_0^{x_F} = 0, \end{aligned}$$

which is valid provided that the volume flux per unit width vanishes at the front and remains finite at the origin.

2.1 Dipole self-similar solution of the first kind

The constancy of the dipole moment throughout the motion suggests that it is possible to find a similarity solution for the motion. This we construct as follows to recover the similarity scalings developed by Barenblatt and Zel'dovich (1957): based on (2.2) and (2.5), scaling arguments indicate that $h^\alpha \sim x^2/\tau$ and $x^2 h \sim \mathcal{M}$, respectively. Eliminating h yields the scale of the length of the current to be

$$x \sim (\mathcal{M}^\alpha \tau)^{\frac{1}{2(\alpha+1)}}. \tag{2.6}$$

Guided by these scalings, we look for a similarity solution of the form

$$h = \left(\frac{\mathcal{M}}{\tau}\right)^{\frac{1}{\alpha+1}} \Psi(\xi), \quad \text{where} \quad \xi = x/(\mathcal{M}^\alpha \tau)^{\frac{1}{2(\alpha+1)}}, \tag{2.7}$$

and where the position of the front is given by $x_F = \zeta_{F0}(M^\alpha \tau)^{1/(2\alpha+2)}$. Substituting this into the governing equation (2.2) yields an ordinary differential equation for Ψ

$$(\alpha + 1)(\Psi^\alpha \Psi')' + \frac{1}{2} \xi \Psi' + \Psi = 0, \tag{2.8}$$

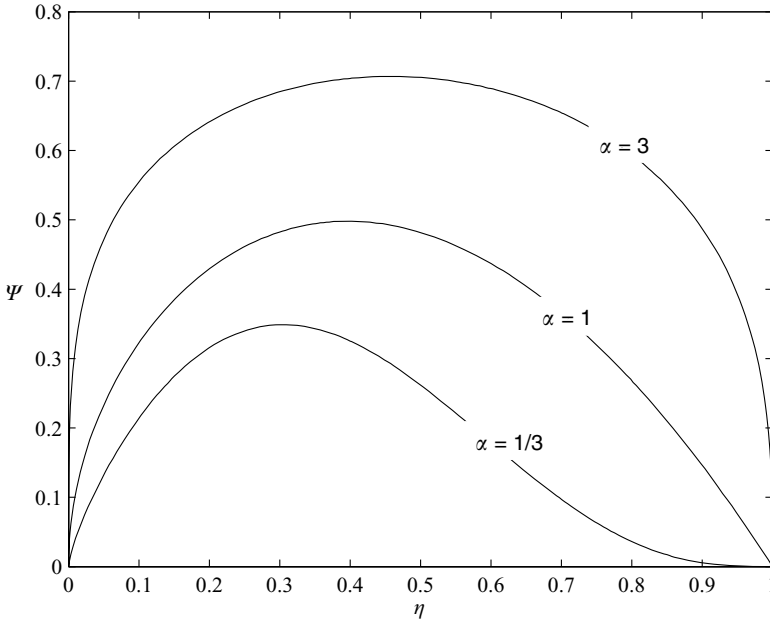


FIGURE 2. The height profiles of the similarity solutions for dipole gravity currents moving through a porous domain, Ψ , plotted as a function of the rescaled similarity variable $\eta = \xi/\xi_{F0}$ for $\alpha = 1/3, 1$ and 3 .

where prime denotes differentiation with respect to ξ . The boundary conditions (2.3)–(2.5) now become

$$\Psi(0) = 0, \quad \Psi(\xi_{F0}) = 0 \quad \text{and} \quad \int_0^{\xi_{F0}} \xi \Psi(\xi) d\xi = 1. \tag{2.9}$$

Multiplying the equation (2.8) by ξ , integrating by parts, and applying the boundary condition (2.9, first condition) give

$$(\alpha + 1)\xi(\Psi^\alpha)' - \alpha\Psi^\alpha + \frac{1}{2}\alpha\xi^2 = 0, \tag{2.10}$$

which is a first-order differential equation in Ψ^α . After a further integration and use of the boundary condition (2.9, second condition), we obtain

$$\Psi^\alpha = \frac{\alpha}{2(\alpha + 2)} (\mathcal{H} \xi^{\frac{\alpha}{\alpha+1}} - \xi^2)_+, \tag{2.11}$$

where $\mathcal{H}^{\alpha+1} = \xi_{F0}^{\alpha+2}$ and $\xi_+ \equiv \max(\xi, 0)$ (Barenblatt and Zel'dovich, 1957). The form of this self-similar solution is shown in Figure 2 for different values of α . The position of the front can now be found by substituting the solution into the integral condition (2.9, third condition), and it is given by

$$\xi_{F0}^{2+2/\alpha} B \left(1 + \frac{1}{\alpha}, \frac{2\alpha + 3}{\alpha + 2} \right) = \left(\frac{\alpha + 2}{\alpha + 1} \right) \left[2 \left(1 + \frac{2}{\alpha} \right) \right]^{1/\alpha}, \tag{2.12}$$

where B denotes the Beta function. Under the similarity solution, the volume per unit width of the current, $V(\tau)$, and the volume flux per unit width of fluid that drains out at $x = 0$, $q(0, \tau)$ are given by

$$V(\tau) = \int_0^{x_F} h(x, \tau) dx = 2\zeta_{F0}^{1+2/\alpha} \left(\frac{\alpha}{2(\alpha+2)} \right)^{\frac{1}{2}+1} \left(\frac{\mathcal{M}^{\alpha+2}}{\tau} \right)^{\frac{1}{2(\alpha+1)}}, \tag{2.13}$$

$$q(0, \tau) = [h^\alpha \partial_x h]_{x=0} = \frac{1}{\alpha+1} \left(\frac{\alpha \mathcal{M}}{2(\alpha+2)} \right)^{\frac{1}{2}+1} \left(\frac{\mathcal{M}^{\alpha+2}}{\tau^{3\alpha+2}} \right)^{\frac{1}{2(\alpha+1)}}. \tag{2.14}$$

The role of the dipole self-similar solution (2.11) as an intermediate asymptotic has been confirmed in laboratory experiments by King and Woods (2003) for flows characterised by $\alpha = 1$ and $\alpha = 3$. They showed that the dipole moment of the flow is conserved and the height profile has the self-similar shape given by (2.11) in the intermediate asymptotic regime. They have also found the predictions given by the analytical expressions for the length of the current, $x_F(t)$, and the volume flux at $x = 0$ (2.14), to be in excellent agreement with their experimental results.

2.2 Linear stability analysis

We study the evolution of the self-similar solution (2.11) subsequent to the introduction of a small perturbation of arbitrary shape. The gradient of the self-similar solution at the moving front is infinite for $\alpha > 1$, and this leads to singular terms in the governing equations of the perturbation function (e.g., Grundy and McLaughlin, 1982; Fowler, 1997). We avoid this problem by employing an approach that was used by Kath and Cohen (1982) to study waiting time properties of non-linear diffusion equations and recently deployed by Mathunjwa and Hogg (2006) to study the stability of other similarity solutions. The dependent variable is transformed so that the height gradient at the moving front remains finite even for $\alpha > 1$. Thus we write

$$\frac{h^\alpha}{\alpha} = \left(\frac{\mathcal{M}}{\tau} \right)^{\frac{\alpha}{\alpha+1}} \Phi(\zeta, \tau), \tag{2.15}$$

where Φ is a rescaled height function in the new system. We note that the gradient of the profile at $\zeta = 0$ is singular even in terms of the new variables but this does not present any difficulties in the analysis that follows because this end of the current is stationary.

Substituting (2.15) into the governing equation (2.2) gives an evolution equation for Φ ,

$$\tau \partial_\tau \Phi = \alpha \Phi \partial_\zeta \partial_\zeta \Phi + (\partial_\zeta \Phi)^2 + \left(\frac{1}{2} \zeta \partial_\zeta \Phi + \alpha \Phi \right) / (\alpha + 1). \tag{2.16}$$

The boundary conditions now take the form

$$\Phi(0, \tau) = 0, \quad \Phi(\zeta_F, \tau) = 0 \quad \text{and} \quad \int_0^{\zeta_F} \zeta (\alpha \Phi)^{\frac{1}{2}} d\zeta = 1. \tag{2.17}$$

We assume that a small disturbance of arbitrary shape is imposed on the self-similar

solution at some reference time $\tau = 1$. To investigate the evolution of the disturbance for times $\tau > 1$, we introduce the expansions

$$\Phi(\xi, \tau) = \Phi_0(\xi) + \delta\Phi_1(\xi, \tau) + \dots, \tag{2.18}$$

$$\xi_F(\tau) = \xi_{F0} + \delta\xi_{F1}(\tau) + \dots, \tag{2.19}$$

where the indices 0 and 1 denote self-similar and leading-order disturbance variables, respectively, and $\delta \ll 1$ is the dimensionless amplitude of the disturbance. These expansions are then substituted into (2.16)–(2.17) and equations governing the self-similar and disturbance quantities are obtained by balancing powers of δ . The governing equation at $O(1)$ is given by

$$\alpha\Phi_0\Phi_0'' + \Phi_0'^2 + (\alpha\Phi_0 + \frac{1}{2}\xi\Phi_0')/(\alpha + 1) = 0, \tag{2.20}$$

and the boundary conditions are $\Phi_0(0) = 0$, $\Phi_0(\xi_{F0}) = 0$, and $\int_0^{\xi_{F0}} \xi(\alpha\Phi_0)^{\frac{1}{\alpha}} d\xi = 1$. It is straightforward to show that this yields the self-similar solution,

$$\Phi_0(\xi) = \frac{1}{2(\alpha + 2)} (\mathcal{K} \xi^{\frac{\alpha}{\alpha+1}} - \xi^2)_+. \tag{2.21}$$

At $O(\delta)$, the perturbation quantity Φ_1 is found to satisfy the partial differential equation,

$$\tau\partial_\tau\Phi_1 = \alpha\Phi_0\partial_\xi\partial_\xi\Phi_1 + \left(2\Phi_0' + \frac{1}{2(\alpha + 1)}\xi\right)\partial_\xi\Phi_1 + \left(\alpha\Phi_0'' + \frac{\alpha}{\alpha + 1}\right)\Phi_1. \tag{2.22}$$

This equation must be solved subject to the boundary conditions,

$$\Phi_1(0, \tau) = 0, \quad \Phi_1(\xi_{F0}, \tau) = \frac{\xi_{F0}\xi_{F1}}{2(\alpha + 1)} \quad \text{and} \quad \int_0^{\xi_{F0}} \xi\Phi_0^{\frac{1}{\alpha}-1}\Phi_1 d\xi = 0, \tag{2.23}$$

where (2.23, first condition) states that the disturbance vanishes at the stationary end, (2.23, second condition) expresses the variation in the position of the moving front caused by the disturbance, and (2.23, third condition) is an expression of conservation of the dipole moment of the perturbation.

Since the governing equation (2.22) is a linear homogeneous PDE of Φ_1 , we look for a solution in separable form

$$\Phi_1(\eta, S) = \sum_{n=0}^{\infty} a_n e^{-\lambda_n S} \mathcal{L}_n(\eta; \lambda_n), \tag{2.24}$$

$$\eta_{F1}(S) = \sum_{n=0}^{\infty} b_n e^{-\lambda_n S}, \tag{2.25}$$

where a_n and b_n are constants to be determined, $\eta = \xi/\xi_{F0}$, $S = \ln \tau$ and λ_n are the eigenvalues of the system. Thus, showing that none of the eigenvalues are negative would prove that the similarity solution (2.11) is linearly stable, provided that the functions \mathcal{L}_n form a complete set.

The eigenfunctions \mathcal{Z}_n satisfy the ordinary differential equation,

$$\eta^2 \left(\eta^{\frac{\alpha}{z+1}} - \eta^2 \right) \mathcal{Z}_n'' + \frac{2}{\alpha+1} \eta \left(\eta^{\frac{\alpha}{z+1}} - \left(\frac{3}{2} + \frac{1}{\alpha} \right) \eta^2 \right) \mathcal{Z}_n' + \frac{2}{\alpha+1} \left(\left[1 + \left(1 + \frac{1}{\alpha} \right) (\alpha+2) \lambda_n \right] \eta^2 - \frac{\alpha}{2(\alpha+1)} \eta^{\frac{\alpha}{z+1}} \right) \mathcal{Z}_n = 0. \tag{2.26}$$

By making the substitutions $\widehat{\zeta} = \eta^{\frac{\alpha+2}{z+1}}$, $\mathcal{Z}_n = \widehat{\zeta}^{\frac{\alpha}{z+2}} Y_n(\widehat{\zeta})$ and $2\widehat{\zeta} = \zeta + 1$ in succession, this equation is transformed into a Jacobi differential equation (Abramowitz and Stegun, 1965),

$$(1 - \zeta^2) Y_n'' + \frac{2}{\alpha(\alpha+2)} [(\alpha^2 + \alpha - 1) - (\alpha+1)^2 \zeta] Y_n' + \frac{2(\alpha+1)^2}{\alpha(\alpha+2)} \lambda_n Y_n = 0, \tag{2.27}$$

defined in $-1 \leq \zeta \leq 1$, where the end points are regular singular points and correspond to $\zeta = 0$ and $\zeta = \zeta_{F0}$. Solutions of this equation that are continuous in the whole interval $-1 \leq \zeta \leq 1$ are given by

$$Y_n(\zeta) = P_n^{(a,b)}(\zeta), \tag{2.28}$$

where $P_n^{(a,b)}$ stands for the Jacobi polynomial of degree n , and $a = (1 - \alpha)/\alpha$, $b = (\alpha + 1)/(\alpha + 2)$. These solutions form a complete set and are characterised by the discrete set of eigenvalues

$$\lambda_n = \frac{n}{2(\alpha+1)^2} [\alpha(\alpha+2)(n+1) + 2], \quad n = 0, 1, 2, \dots \tag{2.29}$$

For positive values of α , all eigenvalues λ_n are nonnegative, indicating that all terms in the disturbance eigenfunction expansion (2.24) decay in time, and hence the self-similar solution (2.11) is stable to small disturbances. The term involving \mathcal{Z}_0 , for which $\lambda_0 = 0$, corresponds to disturbances that alter the dipole moment of the current. We demonstrate below that this term does not invalidate the stability result.

In terms of the rescaled similarity variable η , the eigenfunctions are given by

$$\mathcal{Z}_n(\eta) = \eta^{\frac{\alpha}{z+1}} P_n^{(a,b)}(2\eta^{\frac{\alpha+2}{z+1}} - 1), \tag{2.30}$$

and their structure is illustrated in Figure 3. The boundary condition (2.23, first condition) is automatically satisfied by all eigenfunctions \mathcal{Z}_n . An application of the condition (2.23, second condition) gives

$$b_n = 2a_n(\alpha+1)P_n^{(a,b)}(1)/\zeta_{F0}^2. \tag{2.31}$$

The integral condition (2.23, third condition) is also satisfied by all eigenfunctions \mathcal{Z}_n automatically except \mathcal{Z}_0 . In the next section, we show that this term is equivalent to the coefficient of the infinitesimal symmetry transformation whose action alters the value of the dipole moment of the problem. It will also be shown that the eigenfunction \mathcal{Z}_1 is associated with time-shift transformations.

The solution of the perturbed problem is then given by

$$\Phi(\eta, \tau) = \frac{\zeta_{F0}^2}{2(\alpha+2)} (\eta^{\frac{\alpha}{z+1}} - \eta^2) + \delta \eta^{\frac{\alpha}{z+1}} \sum_{n=0}^{\infty} a_n \tau^{-\lambda_n} P_n^{(a,b)}(2\eta^{\frac{\alpha+2}{z+1}} - 1) + O(\delta^2), \tag{2.32}$$

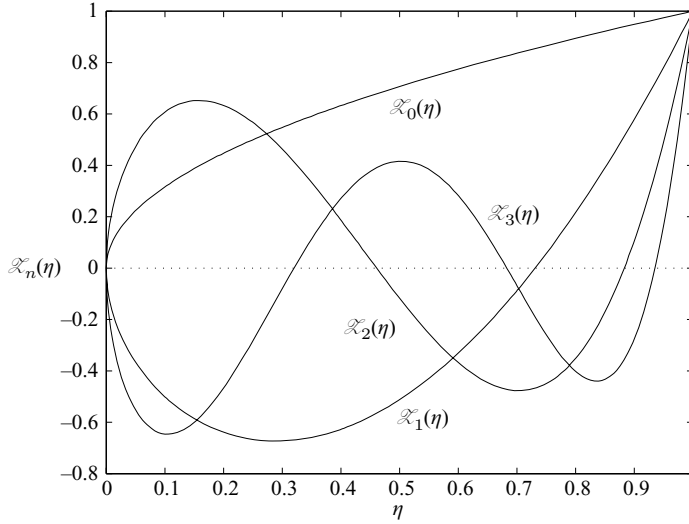


FIGURE 3. The first four eigenfunctions of the disturbance function Φ_1 plotted against $\eta = \xi/\xi_{F0}$ for $\alpha = 1$.

where the constants a_n can be determined from the form of $\Phi_1(\eta, 1)$ by using the properties of orthogonality and completeness of the eigenfunctions.

2.3 Connection with symmetry transformations

The height profiles of currents with different values of \mathcal{M} and currents that evolve from different initial times will all have the same structure in the intermediate regime, given by the self-similar solution (2.11). This is because the solution (2.11) is invariant under the action of transformations that alter the dipole moment \mathcal{M} and shift the origin in time. We demonstrate that the eigenvalues $\lambda_0 = 0$ and $\lambda_1 = 1$ are associated with transformations that alter \mathcal{M} and shift time, respectively. Thus when assessing to which ‘target’ similarity solution a current evolves from non-similarity initial conditions, it is possible to identify a value of the dipole moment and origin in time such that the difference between the solution and the similarity form decays as $\tau^{-\lambda_2}$.

The height profile of the disturbed system is given by

$$h(\eta, \tau) = \left(\frac{\mathcal{M}}{\tau}\right)^{\frac{1}{z+1}} \left[(\alpha\Phi_0)^{\frac{1}{z}} + \delta(\alpha\Phi_0)^{\frac{1}{z}-1} \sum_{n=0}^{\infty} a_n \tau^{-\lambda_n} \mathcal{L}_n(\eta) + O(\delta^2) \right]. \tag{2.33}$$

The first two eigenfunctions, with their respective eigenvalues, are given by

$$\begin{aligned} \mathcal{L}_0(\eta) &= \eta^{\frac{\alpha}{z+1}}, & \lambda_0 &= 0 \\ \mathcal{L}_1(\eta) &= (2 + a + b)\eta^2 - (1 + b)\eta^{\frac{\alpha}{z+1}}, & \lambda_1 &= 1, \end{aligned}$$

where a and b are the parameters of the Jacobi polynomials, defined in equation (2.28). We demonstrate that these eigenfunctions are equivalent to the coefficients of dipole-moment-altering and time-shifting infinitesimal transformations.

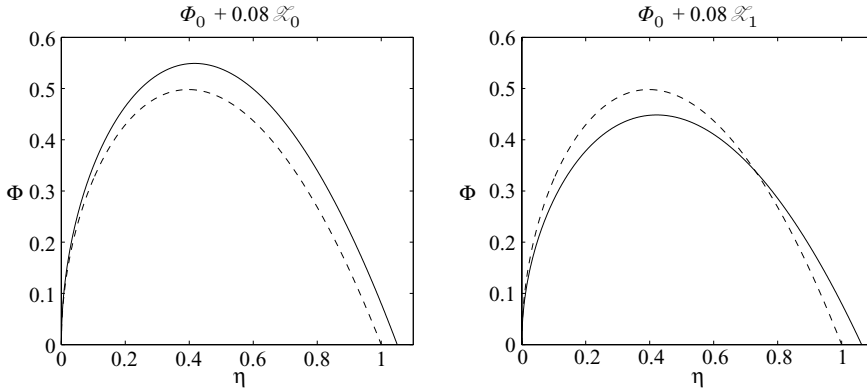


FIGURE 4. The dipole self-similar profile Φ_0 (dashed line) plotted as a function of the rescaled similarity variable η . The perturbed profiles $\Phi_0 + 0.08\mathcal{L}_n$ (solid line) for $n = 0$ and 1 , respectively, are superimposed for comparison. In both cases, $\alpha = 1$.

It is convenient first to write the self-similar solution (2.11) in terms of the primitive variables, as

$$h(x, \tau) = \left[\frac{\alpha}{2(\alpha + 2)} \left[\mathcal{H} x^{\frac{\alpha}{\alpha+1}} \left(\frac{\mathcal{M}^{\alpha(\alpha+2)}}{\tau^{\alpha(2\alpha+3)}} \right)^{\frac{1}{2(\alpha+1)^2}} - \frac{x^2}{\tau} \right] \right]_{+}^{\frac{1}{\alpha}}. \tag{2.34}$$

Transformations that cause a change in the dipole moment of the current are defined by $\mathcal{M} \mapsto \mathcal{M} + \delta$. The image of the self-similar solution (2.34) under the action of such transformations is given by

$$h_{\delta}(x, \tau; \delta) = \left[\frac{\alpha}{2(\alpha + 2)} \left[\mathcal{H} x^{\frac{\alpha}{\alpha+1}} \left(\frac{(\mathcal{M} + \delta)^{\alpha(\alpha+2)}}{\tau^{\alpha(2\alpha+3)}} \right)^{\frac{1}{2(\alpha+1)^2}} - \frac{x^2}{\tau} \right] \right]_{+}^{\frac{1}{\alpha}}. \tag{2.35}$$

The coefficient of the infinitesimal transformation is given by

$$\mathcal{T}_{\delta} = \left[\frac{\partial h_{\delta}}{\partial \delta} \right]_{\delta=0} = \frac{\alpha}{4(\alpha + 1)^2} \mathcal{M}^{\frac{1}{\alpha+1}} (\alpha \Phi_0)^{\frac{1}{\alpha}-1} \eta^{\frac{\alpha}{\alpha+1}} \tag{2.36}$$

and this is equivalent to the first term in the eigenfunction expansion (2.33) of the disturbance function. The effect of adding this eigenfunction onto the self-similar solution is shown in Figure 4 for positive δ , and it resembles that of a transformation that increases the dipole moment of the current.

Time-shift transformations are defined by $\tau \mapsto \tau + \delta$ and the image of the similarity solution under the action of these transformations is given by

$$h_{\delta}(x, \tau) = \left[\frac{\alpha}{2(\alpha + 2)} \left[\mathcal{H} x^{\frac{\alpha}{\alpha+1}} \left(\frac{\mathcal{M}^{\alpha(\alpha+2)}}{(\tau + \delta)^{\alpha(2\alpha+3)}} \right)^{\frac{1}{2(\alpha+1)^2}} - \frac{x^2}{\tau + \delta} \right] \right]_{+}^{\frac{1}{\alpha}}. \tag{2.37}$$

The coefficient of the infinitesimal transformation can now be calculated, and we find

$$\mathcal{T}_\delta = \frac{\alpha}{4(\alpha + 1)^2} \left(\frac{\mathcal{M}}{\tau} \right)^{\frac{1}{\alpha+1}} (\alpha\Phi_0)^{\frac{1}{\alpha}-1} \cdot \frac{1}{\tau} [(2 + a + b)\eta^2 - (1 + b)\eta^{\frac{\alpha}{\alpha+1}}]. \quad (2.38)$$

This expression is equivalent to the second term of the eigenfunction expansion of the disturbance function. In Figure 4, the changes caused by the second eigenfunction on the self-similar profile are shown to resemble those undergone by $h(x, \tau)$ as it evolves in time, characterised by a decrease in height and an increase in length as the profile flattens out.

We have thus shown that the first two eigenfunctions of the disturbance function are equivalent to the coefficients of the infinitesimal transformations that alter the dipole moment of the current and shift the origin in time, respectively. Under the action of these transformations, the problem (2.2)–(2.5) is invariant. Hence, the form of the self-similar solution (2.11) remains the same for different choices of the value of \mathcal{M} and the origin in time. The presence of the first two eigenfunctions in the eigenfunction expansion of Φ_1 is an indication that the inappropriate values of \mathcal{M} and the origin in time have been used. It is always possible to find values of \mathcal{M} and the origin in time (that is, optimal similarity variables) such that the eigenfunction expansion of Φ_1 does not involve \mathcal{L}_0 and \mathcal{L}_1 . This effectively means that the leading-order term of the disturbance function is the \mathcal{L}_2 term for which the rate of decay is $\tau^{-3+1/(\alpha+1)^2}$.

We note that since the similarity solution (2.11) develops in a semi-infinite spatial domain, it is not invariant under the action of spatial translations and hence there is no eigenvalue associated with these transformations.

3 Currents with capillary retention

We now consider the case where the current develops within an unsaturated porous medium. Then, a fraction of the fluid may be retained within the pores by capillary action in the trail of the current (e.g., Bear, 1988). The retention implies that the dipole moment will no longer be conserved and hence the evolution of the height profile will be qualitatively different from that of the case without retention. We assume that the fraction retained, σ , is constant and independent of spatial position. This assumption is reasonable for flows through porous media that possess isotropic homogeneous properties (see, for example, Barenblatt, 1996; Woods, 1988). Thus we consider currents through porous media of constant permeability, that is, the exponent $\alpha = 1$ in this case.

The governing equation now takes the form

$$\partial_x \partial_x \left(\frac{1}{2} h^2 \right) = \begin{cases} (1 - \sigma) \partial_\tau h, & \partial_\tau h < 0, \\ \partial_\tau h, & \partial_\tau h > 0, \end{cases} \quad (3.1)$$

subject to the boundary conditions

$$h(0, \tau) = 0 \quad \text{and} \quad h(x_F, \tau) = 0. \quad (3.2)$$

The dipole moment \mathcal{M} of the current is no longer conserved in time because, in addition to the fluid lost at the origin, fluid loss also occurs because of retention. Thus we write

the dipole moment as $\mathcal{M}(\tau; \sigma)$, with the initial condition that $\mathcal{M}(1; \sigma) = \widehat{\mathcal{M}}$. If we assume that the dipole moment decays according to a power-law dependence on time, then we may write $\mathcal{M}(\tau; \sigma) = \widehat{\mathcal{M}}\tau^{-\gamma}$ – and this is what is done in section 3.1, where the similarity solution of the second kind is constructed and γ is determined as a function of σ .

The basic formulation of the problem presented here was first proposed by Barenblatt and Vazquez (1998). It has also been studied by Ingerman and Shvets (1999), who performed numerical calculations and demonstrated that the intermediate asymptotics of the current are described by a dipole SS2 and by Wagner (2005), who presented an asymptotic means for evaluating γ in the regime $\sigma \ll 1$. We carry out similar calculations here and then, and in section 3.2, use the method of multiple scales to derive leading-order analytic expressions for the dipole SS2.

3.1 Dipole self-similar solution of the second kind

Scaling arguments indicate that the length of the current grows according to $x^4 \sim \widehat{\mathcal{M}}\tau^{1-\gamma}$ and the height decreases according to $h^2 \sim \widehat{\mathcal{M}}\tau^{-(1+\gamma)}$. Thus we write $x_F = A\tau^{(1-\gamma)/4}$ and look for a self-similar solution of the form

$$h(x, \tau; \sigma) = \Pi\tau^{-(1+\gamma)/2}\Phi(\eta), \tag{3.3}$$

where the similarity variable $\eta = x/x_F$, and the constants Π and A , to be determined, will typically depend on $\widehat{\mathcal{M}}$ and the retention parameter σ . We note that the exponents in the similarity variables have been specified as functions of the parameter γ . This parameter is termed the anomalous exponent and it may not be determined by scaling arguments only. This is a hallmark feature of the self-similar solution of the second kind. Substituting into the governing equation (3.1) gives the following ordinary differential equation:

$$(\Phi^2)'' = \begin{cases} (\sigma - 1)[(1 + \gamma)\Phi + \frac{1}{2}(1 - \gamma)\eta\Phi'], & 0 < \eta \leq \eta_S, \\ -[(1 + \gamma)\Phi + \frac{1}{2}(1 - \gamma)\eta\Phi'], & \eta_S < \eta \leq 1, \end{cases} \tag{3.4}$$

where η_S is the point where $(1 + \gamma)\Phi + \frac{1}{2}(1 - \gamma)\eta\Phi' = 0$ and we have assumed that $\Pi = A^2$ without loss of generality. Equation (3.4) must be solved in the interval $0 \leq \eta \leq 1$ subject to the boundary conditions,

$$\Phi(0; \sigma) = 0 \quad \text{and} \quad \Phi(1; \sigma) = 0. \tag{3.5}$$

In addition, since equation (3.4) is degenerate at $\eta = 1$, this implies that

$$\Phi'(1; \sigma) = -\frac{1}{4}(1 - \gamma). \tag{3.6}$$

It is generally impossible to find solutions of the second-order equation (3.4) that satisfy all three boundary conditions (3.5, first and second conditions) and (3.6). There exists, however, a particular value of γ for each σ , at which solutions that satisfy all three boundary conditions may be constructed. We have solved this eigenvalue problem numerically and the variation of the eigenvalues as a function of the level of retention, σ , is shown in Figure 5. Here we plot the exponent $\frac{1}{4}(1 - \gamma)$ as a function of σ ; this exponent occurs

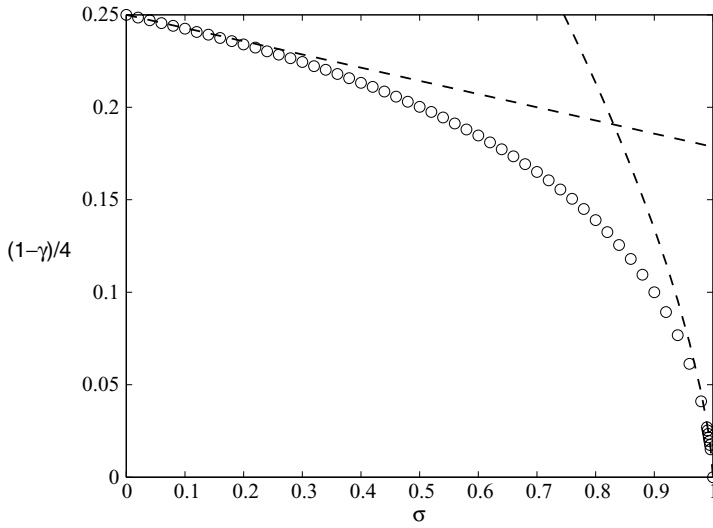


FIGURE 5. The exponent $\frac{1}{4}(1 - \gamma)$ as a function of the retained fraction, σ , calculated numerically (circles) and using asymptotic formulae (dashed curves).

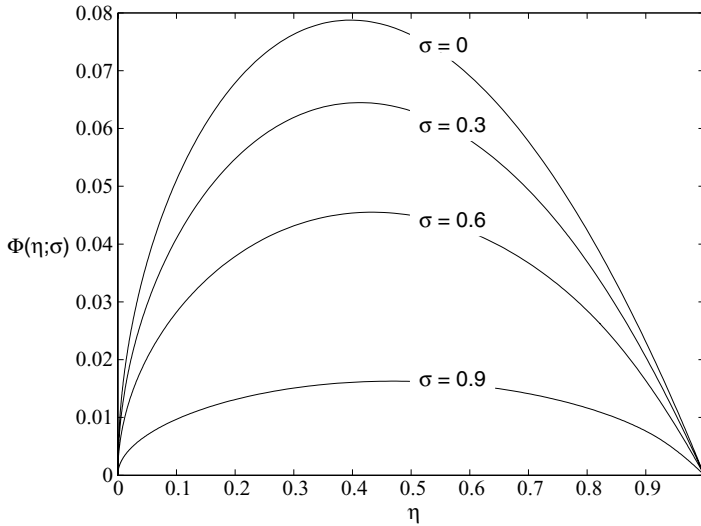


FIGURE 6. Height profiles $\Phi(\eta; \sigma)$ plotted as functions of η for retention levels $\sigma = 0, 0.3, 0.5$ and 0.8 .

in the power-law relationship between x_F and τ . These computations reveal that when none of the fluid is retained ($\sigma = 0$), the anomalous exponent is $\gamma = 0$, yielding $x_F \sim \tau^{1/4}$, in agreement with the SS1 theory (section 2.1). As the fraction retained increases, the exponent $(1 - \gamma)/4$ decreases monotonically reaching 0 at $\sigma = 1$, implying that as more fluid is retained, the rate of advance of x_F decreases, as expected. Figure 6 illustrates the shape of the similarity height function Φ for different retention levels. The shape of $\Phi(\eta)$ is found to become progressively flatter as the fraction retained increases.

It is also possible to analyse the system of equations and boundary conditions (3.4), (3.5, first and second conditions) and (3.6), asymptotically in the regimes of weak retention ($0 < \sigma \ll 1$) and strong retention ($|1 - \sigma| \ll 1$), to determine the anomalous exponent, γ . Using straightforward asymptotic techniques, this yields

$$\gamma = \left(\frac{5}{8}\right)^{8/3} \sigma + \dots, \quad \text{when } 0 < \sigma \ll 1, \tag{3.7}$$

$$\gamma = 1 - 2.494(1 - \sigma)^{2/3} + \dots, \quad \text{when } |1 - \sigma| \ll 1 \tag{3.8}$$

(see the Appendix for this derivation). These asymptotic formulae are plotted in Figure 5, where it can be noted that there is excellent agreement with the numerically calculated values. We note that the result for $\sigma \ll 1$ is identical to that of Wagner (2005), but its calculation here is by a straightforward regular perturbation. We believe that the analysis for $|1 - \sigma| \ll 1$ is new and emerges as a singular perturbation, analysed using matched asymptotic expansions.

It is important to observe that the constants A and Π still remain undetermined. In the problem with no capillary retention (section 2), these constants were evaluated from the integral condition expressing the constancy of the dipole moment. For the present case, the dipole moment of the current is not conserved and so there is no means for generally evaluating A and Π . Rather they are usually found by matching with a numerically calculated solution of the partial differential equations in the transition period from the non-self-similar to the self-similar regime. The behaviour of the system in the transition period is influenced by the details of the initial conditions and, hence in contrast to the SS1 of section 2.1, these constants will depend on the initial conditions of the current. In the following section we develop a technique that avoids the need for this use of numerical solutions and permits the solution to be fully evaluated and related to the initial conditions.

3.2 Weak retention ($\sigma \ll 1$) and the method of multiple scales

It is convenient to express the governing equation (3.1) in the form

$$\partial_\tau h = \partial_x \partial_x \left(\frac{1}{2} h^2\right) + \begin{cases} \epsilon \partial_x \partial_x \left(\frac{1}{2} h^2\right), & 0 \leq x \leq x_S, \\ 0, & x_S \leq x \leq x_F, \end{cases} \tag{3.9}$$

where $\epsilon = \sigma/(1 - \sigma)$ and $x_S(\tau; \epsilon)$ is the point where $\partial_\tau h = 0$. In the regime $\epsilon \ll 1$, it is reasonable to expect the shape of the height profile $h(x, \tau; \epsilon)$ not to deviate much from that of the $\epsilon = 0$ (SS1) case. The dipole moment of the current is no longer constant in time but, with $\epsilon \ll 1$, its rate of temporal variation will be much slower than that of other quantities. In particular, from arbitrary initial conditions, we anticipate that the motion rapidly converges to a similarity solution of the first kind, specified by the dipole moment. Thereafter it progressively evolves away from this state as the effects of retention become significant. To account for the variation of the dipole moment, we introduce a slow time scale $T = \tau^\epsilon$, so that T remains of order unity when $\tau = O(\exp(1/\epsilon))$. We write the dependent variables as functions of this new slow time; importantly, the dipole moment

is now given by $\mathcal{M}(\tau, T; \epsilon)$, where $\mathcal{M} = \widehat{\mathcal{M}}$ at the initial time $\tau = 1$. In terms of the similarity variable $\zeta = x/\tau^{1/4}$, equation (3.9) now becomes

$$\partial_\tau h + \frac{\epsilon T}{\tau} \partial_T h = \frac{\zeta}{4\tau} \partial_\zeta h + \frac{1}{\tau^{1/2}} \partial_\zeta \partial_\zeta \left(\frac{1}{2} h^2 \right) + \begin{cases} \frac{\epsilon}{\tau^{1/2}} \partial_\zeta \partial_\zeta \left(\frac{1}{2} h^2 \right), & 0 \leq \zeta \leq \zeta_S, \\ 0, & \zeta_S \leq \zeta \leq \zeta_F. \end{cases} \quad (3.10)$$

We introduce the expansions

$$h(\zeta, \tau, T; \epsilon) = h_0(\zeta, \tau, T) + \epsilon h_1(\zeta, \tau, T) + \dots, \quad (3.11)$$

$$x_S(\tau, T; \epsilon) = \tau^{1/4} [\zeta_{S0}(T) + \epsilon \zeta_{S1}(T) + \dots], \quad (3.12)$$

$$x_F(\tau, T; \epsilon) = \tau^{1/4} [\zeta_{F0}(T) + \epsilon \zeta_{F1}(T) + \dots], \quad (3.13)$$

while the dipole moment is given by

$$\mathcal{M}(\tau, T; \epsilon) \equiv \int_0^{x_F} xh \, dx = \mathcal{M}_0(T) + \epsilon \mathcal{M}_1(\tau, T) + \dots \quad (3.14)$$

In this expression, we allow the dipole moment formally to be a function of τ and T . However, in anticipation of the leading-order terms in the expansion being the similarity solution for a constant dipole moment, we pose \mathcal{M}_0 as a function of T only.

The multiple scales expansion that follows is based upon preserving the asymptotic ordering of \mathcal{M} , an approach that shares some general features with Wagner (2005). Substituting these expressions into the governing equation (3.10) and balancing powers of ϵ yields, at $O(1)$, the SS1 given by

$$h_0(\zeta, \tau, T) = \frac{1}{6\tau^{1/2}} [\zeta_{F0}^{3/2} \sqrt{\zeta} - \zeta^2], \quad (3.15)$$

where the front is determined from the dipole moment, given by $\zeta_{F0}(T) = [40 \mathcal{M}_0(T)]^{1/4}$ (see section 2.1). This similarity solution (SS1) may not be an appropriate initial condition for the flow. However, we have demonstrated that the similarity solution is linearly stable and thus we anticipate that from given initial conditions, the solution will converge rapidly to this similarity form before appreciable volumes are retained in the pores. This is confirmed through the numerical experimentation reported below (section 4).

At $O(\epsilon)$, the governing equation for h_1 is given by

$$6\tau \partial_\tau h_1 - \frac{3}{2} \zeta \partial_\zeta h_1 - \partial_\zeta \partial_\zeta [(\zeta_{F0}^{3/2} \sqrt{\zeta} - \zeta^2) h_1] = -\frac{6\mathcal{R} \sqrt{\zeta}}{\tau^{1/2}} + \begin{cases} \frac{1}{\tau^{1/2}} (\zeta^2 - \frac{5}{8} \zeta_{F0}^{3/2} \sqrt{\zeta}), & 0 \leq \zeta \leq \zeta_{S0}, \\ 0, & \zeta_{S0} \leq \zeta \leq \zeta_{F0}, \end{cases} \quad (3.16)$$

where $\mathcal{R} = 5T(d\mathcal{M}_0/dT)/[2(40\mathcal{M}_0)^{5/8}]$ and $\zeta_{S0} = \zeta_{F0} \ell/4$, where $\ell = 5^{1/3}$. We may integrate (3.16) to deduce the following equation for the first-order perturbation to the dipole

moment:

$$\partial_\tau \mathcal{M}_1 = \frac{1}{6\tau} \left[\int_0^{\zeta_{F0}} -6\mathcal{R}\zeta^{3/2} d\zeta + \int_0^{\zeta_{S0}} \zeta^3 - \frac{5}{8}\zeta_{F0}^{3/2}\zeta^{3/2} d\zeta \right]. \tag{3.17}$$

Thus, to ensure that \mathcal{M}_1 does not grow as $\log \tau$, we require that the right-hand side of (3.17) vanishes and thus \mathcal{M}_1 is a function only of T . This yields

$$\mathcal{R} = -\frac{25}{4096}\ell^2\zeta_{F0}^{3/2}. \tag{3.18}$$

We may construct the complete solution to (3.16) by writing $h_1 = \sqrt{\zeta}\mathcal{F}(\zeta, T)/\tau^{1/2}$ and changing the dependent variable so that $\mathcal{X}^2 = \zeta/\zeta_{F0}$, noting that $\mathcal{X}_{S0}^2 = \ell^2/4$. The solution of this equation in the region $0 \leq \mathcal{X} \leq \mathcal{X}_{S0}$ that remains bounded at $\mathcal{X} = 0$ is given by

$$\mathcal{F}_R(\mathcal{X}, T) = \frac{1}{6}\zeta_{F0}^{3/2}\mathcal{X}^3 - \frac{8\mathcal{R}}{5}\ln(1 - \mathcal{X}^3) + C_1. \tag{3.19}$$

In the frontal region $\mathcal{X}_{S0} \leq \mathcal{X} \leq 1$, the solution that remains bounded at $\mathcal{X} = 1$ is given by

$$\mathcal{F}_F(\mathcal{X}, T) = \frac{12\mathcal{R}}{5\mathcal{X}^2} - \frac{12\mathcal{R}}{5} \left[\ln(1 + \mathcal{X} + \mathcal{X}^2) + \frac{2}{\sqrt{3}} \tan^{-1} \left(\frac{2\mathcal{X} + 1}{\sqrt{3}} \right) \right] + C_2. \tag{3.20}$$

The unknowns, C_1 and C_2 , are determined by requiring that the height of the fluid layer and the volume flux are continuous at $\mathcal{X} = \mathcal{X}_{S0}$. These two conditions yield

$$C_1 = -\frac{125}{768}\zeta_{F0}^{3/2} + \frac{5\ell^2}{512}\zeta_{F0}^{3/2} \left[\sqrt{3} \tan^{-1} \left(\frac{1 + \ell}{\sqrt{3}} \right) + \frac{3}{2} \ln \left(\frac{4 + 2\ell + \ell^2}{3^{2/3}} \right) \right] + C_2,$$

$$C_2 = -\frac{5\ell^2}{512}\zeta_{F0}^{3/2} \left[\frac{\pi}{2\sqrt{3}} + \ln(72) - \frac{507}{120} \right].$$

Notice that the solution $\mathcal{F}(\eta, T)$ has the form $[\zeta_{F0}(T)]^{3/2}\mathcal{G}(\eta)$, where $\eta = \zeta/\zeta_{F0}$ and the function \mathcal{G} is determined from (3.19) and (3.20). Thus the deviation of the height field from the leading-order similarity solution (SS1) is given by

$$h_1(\eta, \tau, T) = \frac{[\zeta_{F0}(T)]^2}{\tau^{1/2}} \sqrt{\eta}\mathcal{G}(\eta) = \left[\frac{40\mathcal{M}_0(T)}{\tau} \right]^{\frac{1}{2}} \Omega(\eta), \tag{3.21}$$

where $\Omega(\eta) = \sqrt{\eta}\mathcal{G}(\eta)$, and its form is plotted in Figure 7.

As a final step we use the expression for $\mathcal{R}(T)$ to find the evolution of the dipole moment in terms of the slow timescale. This yields

$$\frac{d\mathcal{M}_0}{dT} = -\frac{25\ell^2}{256} \frac{\mathcal{M}_0}{T}. \tag{3.22}$$

Thus, we find that the dipole moment is given by

$$\mathcal{M}_0(T; \epsilon) = \widehat{\mathcal{M}} T^{-25\ell^2/(256)}, \tag{3.23}$$

and by combining this with the formula (2.13) for the volume in the current yields the

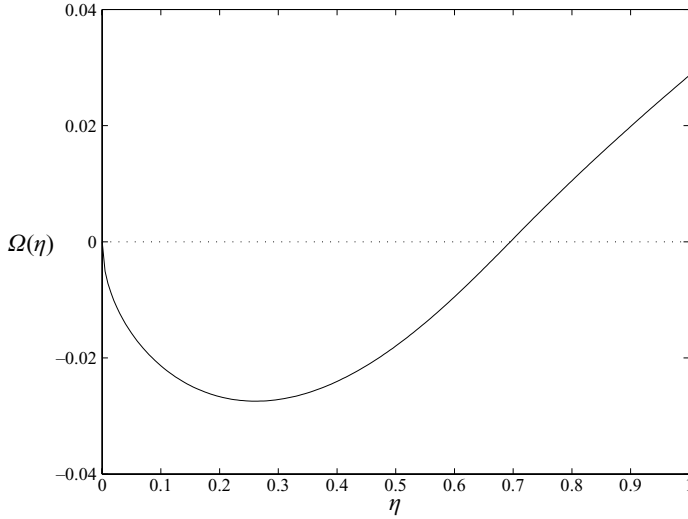


FIGURE 7. The function $\Omega(\eta)$ (which characterises the structure of the first-order deviation term h_1 from the SS1 height profile for a gravity current with retention parameter $\epsilon \ll 1$) plotted as a function of η .

following leading-order expression

$$V(\tau; \epsilon) = \frac{(40\widehat{\mathcal{M}})^{\frac{3}{4}}}{18} \tau^{-\frac{1}{4}(1+75\ell^2\epsilon/(256))}. \tag{3.24}$$

Comparing the formula (3.23) with the power-law relation $\mathcal{M}(\tau; \epsilon) = \widehat{\mathcal{M}}\tau^{-\gamma}$ indicates that the anomalous exponent γ is given by

$$\gamma = \frac{25\ell^2}{256}\epsilon + O(\epsilon^2). \tag{3.25}$$

The values of the exponent $\frac{1}{4}(1 - \gamma)$ generated by this formula are compared with numerically calculated values in Figure 5. The plots show that the asymptotic estimates are in good agreement with the numerical values in the regime $\sigma \ll 1$. Indeed this estimate derived using a multiple-scales analysis of the governing partial differential equation is equal to that derived from direct asymptotic analysis of the ordinary differential that governs the form of the similarity solution (see the Appendix and Wagner, 2005). The advantage with the multiple-scales approach is that it is possible to make a connection with initial conditions, rather than patching to the solutions numerically.

We now calculate the leading-order expression for the position of the front of the SS2 current. Expanding (3.23) in powers of ϵ and substituting into the expression for ζ_{F0} give

$$x_F(\tau; \epsilon) = \tau^{\frac{1}{4}} \left[\hat{\zeta}_{F0} + \epsilon \left(\zeta_{F1} - \frac{25\ell^2}{1024} \hat{\zeta}_{F0} \ln \tau \right) \right] + O(\epsilon^2), \tag{3.26}$$

where $\hat{\zeta}_{F0} = (40\mathcal{M}_0)^{1/4}$. Then, evaluating the height at $x = x_F$ using the expressions (3.15)

and (3.20) for h_0 and h_1 , respectively, gives, at $O(\epsilon)$,

$$\zeta_{F1} = \frac{5\ell^2}{256} \hat{\zeta}_{F0} \left(\frac{\pi}{\sqrt{3}} + \frac{507}{60} - \ln(576) - 3 \right). \tag{3.27}$$

The leading-order expression for the position of the front of the current is thus given by

$$x_F(\tau; \epsilon) = \hat{\zeta}_{F0} \tau^{\frac{1}{4}(1-25\ell^2\epsilon/(256))} \left[1 + \frac{5\ell^2}{256} \epsilon \left(\frac{\pi}{\sqrt{3}} + \frac{507}{60} - \ln(576) - 3 \right) \right] + \dots \tag{3.28}$$

The exponent of τ in this expression is less than $\frac{1}{4}$, indicating that the rate of advance of the front is slower for the SS2 current than for the SS1 current. We remark that the expansion (3.26) remains asymptotic, and hence (3.28) is valid, only for times $\tau < \exp\left(\frac{1024}{25\ell^2\epsilon}\right)$.

4 Numerical solution

We have performed numerical integrations of the governing partial differential equations with and without retention, having first re-mapped them onto a stretched spatial domain, $x/x_F(t)$, which ranged between 0 and 1. To this end we adopted a forward-in-time, centred-in-space finite difference scheme. This scheme was validated using the similarity solution presented in section 2.1 and for other initial conditions without retention it was found that the dipole moment was conserved to within 10^{-4} for computations with 100 grid points and over times that led to the results presented below. The scheme is explicit and so there is a need to take a relatively small time step in order to maintain numerical stability, but this did not lead to prohibitively long computations.

In all calculations reported here, the parameter $\alpha = 1$ and the initial height profile were given by

$$h(\eta, 1) = \left(\frac{45}{8}\right)^{1/2} (\eta^{1/2} - \eta) \quad \text{and} \quad x_F(1) = 40^{1/4}, \tag{4.1}$$

where $\eta = x/x_F$. This initial condition was chosen so that the initial dipole moment is unity ($\mathcal{M}(1; \epsilon) = 1$). Moreover, the form of the initial distribution in the regime $\eta \ll 1$ was chosen so that the volume flux at the origin was initially finite, but nonzero. Other forms of initial profile close to the origin lead to either a delay before the current starts draining from $x = 0$ or very rapid initial drainage. The chosen initial profile was used to examine convergence to the similarity solution in the case of no retention and to the solution developed in section 3.2 when there is retention. Our numerical experimentation found that the presented results are typical of those for a wide range of initial conditions.

We first consider the behaviour in the absence of capillary retention. In Figure 8(a) and (b), we plot the numerically computed position of the front and the volume of the current as functions of time. In these figures, we have also plotted the similarity solution and we note that the computed solution rapidly converged to the similarity expression. We confirm this observation by considering the decay of the difference between the computed and similarity positions of the front. We define

$$D_F(\tau) = \left| 1 - \frac{x_F(\tau)}{(40 \cdot \mathcal{M}(\tau))^{1/4}} \right|, \tag{4.2}$$

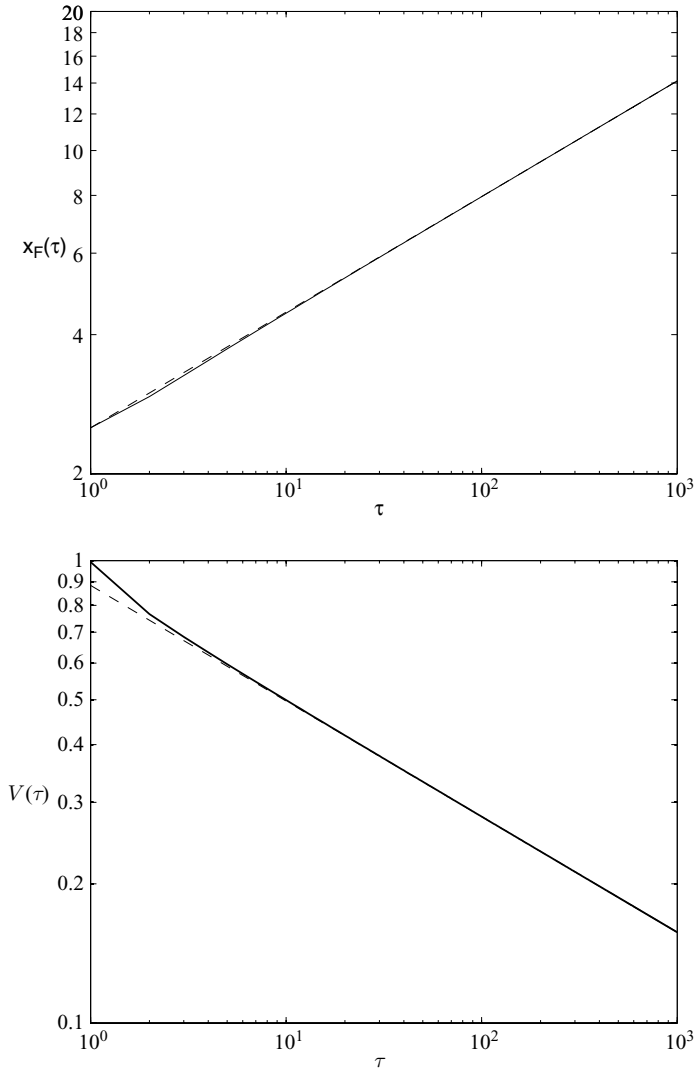


FIGURE 8. (a) The position of the front, x_F , and (b) the volume of the fluid per unit width, $V(\tau)$ as a function of time, τ . The numerically calculated position is plotted with a solid line; the similarity solution is plotted with a dashed line.

and plot the evolution of $D_F(\tau)$ in Figure 9. We observe that the difference between the the similarity solution and the computed solution decays in proportion to $1/\tau$ in accord with the linear stability calculation of section 2.3, which reveals that this is the most slowly decaying eigenfunction. Moreover we may write the initial condition in terms of the eigenfunctions,

$$\left(\frac{45}{8}\right)^{1/2} (\eta^{1/2} - \eta) = \frac{(40)^{1/2}}{6} (\eta^{1/2} - \eta^2) + \sum_{n=1}^{\infty} a_n \eta^{1/2} P_n^{(0,2/3)} (2\eta^{3/2} - 1), \quad (4.3)$$

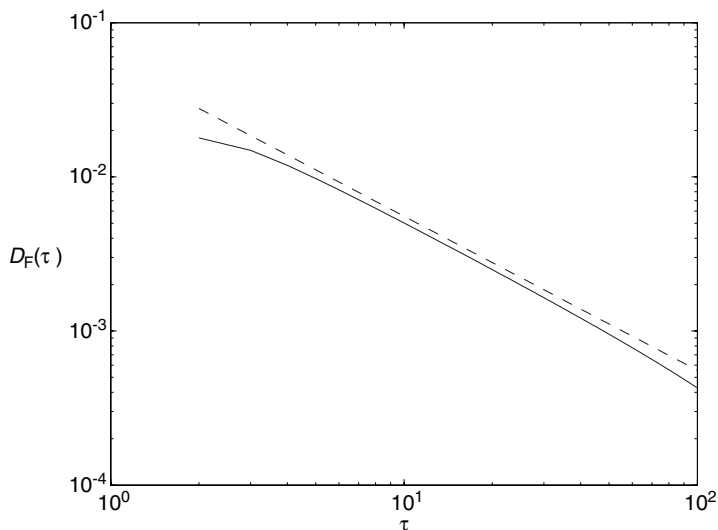


FIGURE 9. The normalised difference in length of the current, arising from the non-similarity initial condition, and the similarity solution for the position of the front, $D_F(\tau)$ as a function of time, τ . The solid line shows the numerically computed value, and the dashed line shows the prediction of the long-term decay on the basis of linear stability analysis.

and find that $a_1 = (10)^{1/2}/36$. Thus, on the basis of the linear stability analysis, we expect

$$D_F(\tau) = \frac{1}{18\tau} + \dots \quad \text{when} \quad \tau \gg 1. \tag{4.4}$$

We note from Figure 9 that this prediction shows reasonably good agreement with the computations, even though the initial difference between the profile and the similarity solution is not small.

We now consider the evolution of the current when there is retention and for this computation we set $\epsilon = 0.1$. In Figure 10, we plot the evolution of length, volume and dipole moment of the current, noting that in contrast to the currents without retention, the dipole moment is progressively reducing. We also plot the asymptotic expressions for these quantities derived in section 3.2, and we note that there is very close correspondence between them. In these asymptotic expressions, there are no adjustable parameters. The computed solution, although not initially in similarity form, rapidly approaches the similarity form before significant volumes of fluid are lost through retention. Thereafter the flow evolves, losing fluid through drainage at $x = 0$ and through retention – and the asymptotic predictions of the form of solution are shown to work well.

5 Concluding remarks

We have analysed the two-dimensional motion of finite-volume gravity currents that propagate through porous media with and without capillary retention, while fluid simultaneously drains out freely from one end. The intermediate asymptotic development of currents that flow without retention through porous media with permeability that may

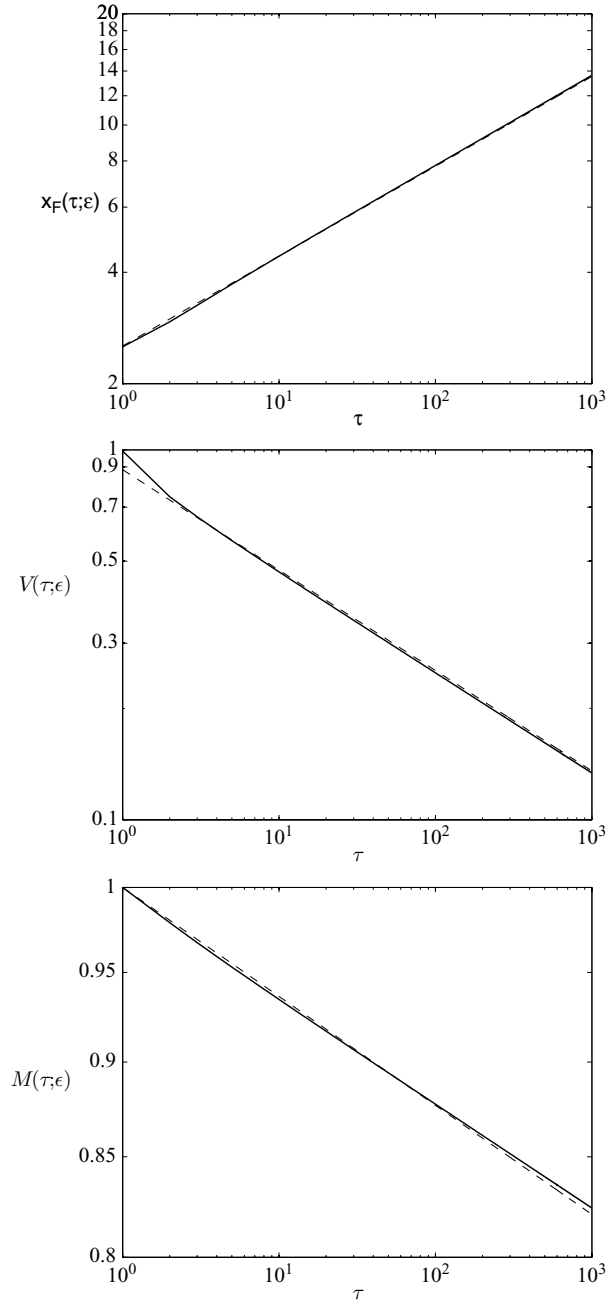


FIGURE 10. (a) The position of the front, $x_F(\tau; \epsilon)$; (b) the volume of the fluid per unit width, $V(\tau; \epsilon)$; and (c) the dipole moment of the current, $M(\tau; \epsilon)$, as functions of time, τ , when there is capillary retention ($\epsilon = 0.1$). The numerically calculated values are plotted with a solid line; the asymptotic solutions are plotted with a dashed line.

vary with height is described by a family of dipole similarity solutions of the first kind. We have shown that small perturbations of arbitrary shape, imposed on the dipole SS1, decay in time, and therefore the dipole SS1 are linearly stable. By demonstrating the relationship between the perturbation eigenfunctions and symmetry transformations of the dipole SS1, we have shown that variables can always be found in terms of which the leading-order rate of decay of the perturbation is maximised. These results complement the work of King and Woods (2003), in which the theoretical predictions of the dipole SS1 are shown to be in excellent agreement with experimental evidence, and thus firmly establish the role of dipole SS1 as intermediate asymptotics for the currents under consideration.

Currents for which a constant fraction of fluid is retained within the homogeneous porous medium as they spread out are modelled by dipole similarity solutions of the second kind in the intermediate asymptotic regime. SS2 are characterised by anomalous exponents that may be found by numerically solving eigenvalue problems, and hence the conventional procedure of finding SS2 generally involves a combination of analytic and numerical techniques. We have developed an approach that fully determines the evolution towards the SS2 through analytic means without the need to supplement with numerical calculations. Using the method of multiple scales, we have derived leading-order analytic expressions for the dipole SS2 parameters, including the anomalous exponent, valid in the regime when the fraction retained is small. The theoretical predictions of the rate of decay of the volume and the rate of advance of the position of the front of the current obtained using these expressions have been compared with the results of numerical integration of the governing equations and have been shown to be very accurate.

We conclude by commenting that the techniques developed here may be more widely applied to other flows. Firstly we have shown how to determine the linear stability properties of similarity solutions when there is a moving front at which the solution exhibits mildly singular behaviour and the governing equation is degenerate. In this case the gradient of the height of the current diverged as the front was approached and this was resolved by appropriate transformations of the dependent and independent variables that then permitted straightforward, and in this case analytical, exploration of the linear stability.

We have also shown how to analyse systematic gradual divergence from a similarity solution when a new physical process influences the motion. (In this study, it was capillary retention within the unsaturated porous medium.) We have analysed this effect by applying the method of multiple scales, where the time scale of the new physical process is much longer than that of the rest of the flow. Thus we were able to capture the progressive divergence from a similarity solution of the first kind to a similarity solution of the second kind – and we suggest that this technique may be applicable in many other scenarios.

Appendix

In this appendix we analyse the eigenvalue problem that determines the anomalous exponent, γ , given by (3.4) with boundary conditions (3.5)–(3.6), in the regimes of weak retention, $0 < \sigma \ll 1$ and strong retention, $0 < 1 - \sigma \ll 1$, of fluid within the initially dry pores of the porous domain. In this analysis, we determine the leading-order expression for the exponent, γ .

1 Weak retention: $\sigma \ll 1$

We substitute $\sigma = \delta$ and use $\delta \ll 1$ as the ordering parameter. We seek a solution of the form

$$\Phi(\eta) = \Phi_0(\eta) + \delta\Phi_1(\eta) + \dots \quad \text{and} \quad \gamma = \delta\gamma_1 + \dots, \tag{A1}$$

where the similarity function, $\Phi_0 = (\eta^{1/2} - \eta^2)/6$, is the leading-order expression for the height fields, derived using the constancy of the dipole moment (section 2.1). We substitute these power series expansions, (A1), into the governing equation (3.4) and at $O(\delta)$ find that

$$2(\Phi_0\Phi_1)'' + \frac{1}{2}\eta\Phi_1' + \Phi_1 = \gamma_1 \left(\frac{1}{2}\eta\Phi_0' - \Phi_0 \right) + \begin{cases} \Phi_0 + \frac{1}{2}\eta\Phi_0' & (\Phi^2)'' > 0, \\ 0 & (\Phi^2)'' < 0, \end{cases} \tag{A2}$$

with boundary conditions $\Phi_1(0) = 0$, $\Phi_1(1) = 0$ and $\Phi_1'(1) = \gamma_1/4$. It is sufficient at this order to apply these two forms of the governing equation in the domains $0 \leq \eta < \eta_{s0}$ and $\eta_{s0} < \eta < 1$, where $\eta_{s0} = 5^{2/3}/4$. At $\eta = \eta_{s0}$, we require that the mass flux and pressure are continuous, which demands that both Φ and Φ' are continuous at $\eta = \eta_{s0}$.

We integrate (A2) analytically to find that when $\eta < \eta_{s0}$

$$\Phi_1 = \frac{\eta^2}{6} + \frac{\gamma_1\eta^{1/2}}{10} \ln(1 - \eta^{3/2}) + C\eta^{1/2}, \tag{A3}$$

where C is a constant. This expression satisfies $\Phi_1(0) = 0$. Also we find that when $\eta > \eta_{s0}$

$$\Phi_1 = \frac{3\gamma_1\eta^{1/2}}{20} \left[-\frac{1}{\eta} + \ln\left(\frac{1 + \eta^{1/2} + \eta}{3e^{-1}}\right) + \frac{2}{\sqrt{3}} \tan^{-1}\left(\frac{2\eta^{1/2} + 1}{\sqrt{3}}\right) - \frac{2\pi}{3\sqrt{3}} \right], \tag{A4}$$

where this expression satisfies $\Phi_1(1) = 0$. Finally matching the mass flux and pressure at the interface between the two regions determines the unknown γ_1 and C and thence we deduce that

$$\gamma = \left(\frac{5}{8}\right)^{8/3} \sigma + \dots \quad \text{when} \quad \sigma \ll 1. \tag{A5}$$

2 Strong retention: $|1 - \sigma| \ll 1$

We now write $\tilde{\delta} = 1 - \sigma$ and examine the eigenvalue problem in the regime $0 < \tilde{\delta} \ll 1$. We seek a solution for the eigenvalue of the form

$$\gamma = 1 - A\tilde{\delta}^a, \tag{A6}$$

where A and a are positive constants to be determined.

We first examine the governing equation (3.4) in the region $\eta_s \leq \eta \leq 1$. We substitute $\Phi = A^2\tilde{\delta}^{2a}\Psi$ and $\eta = 1 - A\tilde{\delta}^a s$ to find that

$$\frac{d^2}{ds^2}(\Psi^2) = (-2 + A\tilde{\delta}^a)\Psi + \frac{1}{2}(1 - A\tilde{\delta}^a s)\frac{d\Psi}{ds}, \tag{A7}$$

subject to $\Psi = 0$ and $d\Psi/ds = \frac{1}{4}$ at $s = 0$. We expand $\Psi = \Psi_0 + \tilde{\delta}\Psi_1 + \dots$ and thus to

leading order

$$\frac{d^2\Psi_0}{ds^2} - \frac{1}{2}\frac{d\Psi_0}{ds} + 2\Psi_0 = 0. \tag{A8}$$

Integrating this differential equation numerically, we find that $4\Psi_0 = d\Psi_0/ds$ at $s \equiv s_* = 0.1857$ and $\Phi_0(s_*) \equiv \Phi_* = 0.03736$ and this evaluates η_s . Therefore, to leading order we find that

$$\eta_s = 1 - 0.1857 A\tilde{\delta}^a \quad \text{and} \quad \Phi(\eta_s) = \Phi_* A^2\tilde{\delta}^{2a}. \tag{A9}$$

We now consider the governing equation in the region $0 \leq \eta \leq \eta_s$ and substitute $\Phi = \tilde{\delta}\sqrt{\psi}$ to find that

$$\psi'' = -(2 - A\tilde{\delta}^a)\sqrt{\psi} - \frac{1}{4}A\tilde{\delta}^a\eta\psi'/\sqrt{\psi}, \tag{A10}$$

subject to $\psi(0) = 0$, $\psi(\eta_s) = \Phi_*^2 A^4 \tilde{\delta}^{4a-2}$ and $\psi'(\eta_s) = 8\Phi_*^2 A^3 \tilde{\delta}^{3a-2}$. Thus we deduce the distinguished scaling $a = \frac{2}{3}$ and by writing $\psi = \psi_0 + \tilde{\delta}\psi_1 + \dots$, find that to leading order

$$\psi_0'' + 2\sqrt{\psi_0} = 0, \tag{A11}$$

subject to $\psi_0(0) = 0$ and $\psi_0(1) = 0$. The non-trivial solution to this system has a non-vanishing gradient at $\eta = 1$. Matching this to the conditions derived above determines the constant A , which is given by

$$\psi_0'(1) = -\frac{3}{[B(\frac{1}{2}, \frac{2}{3})]^3} = 8\Phi_*^2 A^3. \tag{A12}$$

Hence we find that

$$\gamma = 1 - 2.494(1 - \sigma)^{2/3} + \dots \quad \text{when} \quad |1 - \sigma| \ll 1. \tag{A13}$$

References

ABRAMOWITZ, M. & STEGUN, I. A. (1965) *Handbook of Mathematical Functions*, Dover Publications Inc.

BARENBLATT, G. I. (1996) *Scaling, Self-Similarity, and Intermediate Asymptotics*, Cambridge University Press.

BARENBLATT, G. I., INGERMAN, E. A., SHVETS, H. & VAZQUEZ, J. L. (2000) Very intense pulse in the groundwater flow in fissurized-porous stratum. *Proc. Nat. Acad. Sci. U.S.A.* **97**(4), 1366–1369.

BARENBLATT, G. I. & VAZQUEZ, J. L. (1998) A new free boundary problem for unsteady flows in porous media. *Eur. J. Appl. Math.* **9**, 37–54.

BARENBLATT, G. I. & ZEL'DOVICH, YA. B. (1957) On dipole solutions in problems on non-stationary filtration of gas under polytropic regime. *Prikladnaia Matematika i Mekhanika* **21**(5), 718–720.

BEAR, J. (1988) *Dynamics of Fluids in Porous Media*, Dover.

BERNIS, F., HULSHOF, J. & KING, J. R. (2000) Dipoles and similarity solutions of the thin film equation in the half-line. *Nonlinearity* **13**, 413–439.

BOWEN, M. & WITELSKI, T. P. (2006) The linear limit of the dipole problem for the thin film equation. *SIAM J. Appl. Math.* **66**, 1727–1748.

FOWLER, A. C. (1997) *Mathematical Models in the Applied Sciences*, Cambridge University Press.

- GOLDENFELD, N., MARTIN, O., OONO, Y. & LIU, F. (1990) Anomalous dimensions and the Renormalization Group in a nonlinear diffusion process. *Phys. Rev. Lett.* **64**, 1361–1364.
- GRUNDY, R. E. & MCLAUGHLIN, R. (1982) Eigenvalues of the Barenblatt–Pattle similarity solution in nonlinear diffusion. *Proc. Royal. Soc. Lond. Ser. A* **383**, 89–100.
- HUPPERT, H. E. & WOODS, A. W. (1995) Gravity-driven flows in porous layers. *J. of Fluid Mech.* **292**, 53–69.
- INGERMAN, E. A. & SHVETS, H. (1999) *Numerical Investigation of the Dipole Type Solution for the Unsteady Groundwater Flow With capillary Retention and Forced Drainage*, Centre for Pure and Applied Mathematics, University of California, Berkeley, CPAM–775.
- KATH, W. L. & COHEN, D. S. (1982) Waiting-time behaviour in a nonlinear diffusion equation. *Stud. Appl. Math.* **67**, 79–105.
- KING, S. E. & WOODS, A. W. (2003) Dipole solutions for viscous gravity currents: Theory and experiments. *J. Fluid Mech.* **483** 91–109.
- MATHUNJWA, J. S. & HOGG, A. J. (2006) Self-similar gravity currents in porous media: Linear stability of the Barenblatt–Pattle solution revisited. *Eur. J. Mech. B Fluids* **25**, 360–378.
- WAGNER, B. (2005) An asymptotic approach to second-kind similarity solutions of modified porous-medium equation. *J. Eng. Math.* **53**, 201–220.
- WOODS, A. W. (1998) Vapourizing gravity currents in a superheated porous medium. *J. Fluid Mech.* **377**, 151–168.